Earthquake Engineering & Structural Dynamics

WILEY

RESEARCH ARTICLE

Quantifying the Impacts of Incorporating Damage Correlation on Scenario-Based Regional Seismic Assessment

Tomas Mejia | Gerard J. O'Reilly

Centre for Training and Research on Reduction of Seismic Risk (ROSE Centre), Scuola Universitaria Superiore IUSS Pavia, Pavia, Italy

Correspondence: Gerard J. O'Reilly (gerard.oreilly@iusspavia.it)

Received: 17 April 2025 | **Revised:** 11 September 2025 | **Accepted:** 15 September 2025

Funding: The work presented in this paper has been developed within the framework of the project "Dipartimenti di Eccellenza 2023–2027," funded by the Italian Ministry of Education, University and Research at IUSS Pavia. The NLTH analyses were carried out on the High Performance Computing DataCenter at IUSS, co-funded by Regione Lombardia through the funding programme established by Regional Decree No. 3776 of November 3, 2020.

Keywords: damage correlation | PBEE | regional assessment | scenario analysis

ABSTRACT

One of the key challenges in applying the performance-based earthquake engineering framework at a regional scale is accounting for structure-to-structure damage correlation, which is commonly neglected in regional risk assessment. This correlation reflects the tendency for buildings in the same area, often constructed with similar materials, design practices, and vulnerabilities, to exhibit similar damage states after an earthquake. In this study, damage correlation was estimated using a method based on correlated Bernoulli trials, with marginal and joint damage probabilities derived from non-linear time history analyses. Specifically, multiple stripe analysis on detailed 3D building models and incremental dynamic analysis on equivalent single-degree-of-freedom oscillators were employed to obtain these probabilities. To evaluate the implications of incorporating this correlation in regional analysis, a case study was conducted on mid-rise reinforced concrete frame buildings in the province of Caserta, Italy. Results show that while the inclusion of correlation has little impact on the mean and median estimates of damaged buildings for a given scenario, it significantly influences the dispersion and tail behaviour of the damage distribution, increasing the likelihood of widespread damage. These findings highlight the importance of accounting for damage correlation in regional seismic risk analyses to support more accurate loss estimates and better-informed mitigation strategies.

1 | Introduction

The quantification of seismic risk has gained significant interest among practitioners and researchers in the field of earthquake engineering in recent decades. This was primarily through the development of performance-based earthquake engineering (PBEE), originally defined in the SEAOC's Vision 2000 document, and later refined by Cornell and Krawinkler [1] through what became known as the Pacific Earthquake Engineering Research Center (PEER) PBEE framework, which was later formulated into a practical performance assessment methodology via FEMA P-58 [2]. In the framework of PBEE, different efforts have been made to develop practical probabilistic methodologies for assessing and designing structures, starting with the works of Cornell et al. [3] and different studies developed to improve that methodology by Vamvatsikos [4], among many others. In this context, the risk integral was a key component to evaluate performance and is given as:

$$\lambda(DS) = \int_0^{+\infty} P(D > C|IM)\,|dH(IM)| \tag{1}$$

where $\lambda(DS)$ is the mean annual frequency of exceedance for a certain damage state (DS), such as light damage or collapse of a

Summary

- The impact of incorporating building-to-building damage correlation in scenario-based regional seismic assessments is investigated—a factor often neglected or oversimplified.
- A case study in southern Italy is used to apply the proposed methodology, estimating correlation via correlated Bernoulli trials and joint damage probabilities derived from non-linear time history analyses.
- Results demonstrate that accounting for damage correlation significantly affects damage estimates, laying the groundwork for scalable applications in future large-scale seismic risk assessments.

structure, C and D are scalar values that represent, respectively the capacity and demand characterised in terms of engineering demand parameters (EDP), and $dH(IM)$ is the derivative of the hazard curve estimated through probabilistic seismic hazard analysis (PSHA) for a given seismic intensity measure (IM). When $D > C$, the case when the considered DS has been exceeded is represented, and the corresponding intensity at which this occurred can be defined in terms of the chosen IM (e.g., the spectral acceleration for the fundamental period, $Sa(T_1)$). When utilising several ground motions, the so-called record-to-record variability in characterising the DS becomes evident, and the IM level to exceed DS is defined probabilistically via a fragility function as $P(D > C|IM)$.

Although many risk assessment methodologies were developed and widely implemented worldwide for individual buildings (e.g., in refs. [5–7]), it is arguably more important from a societal perspective to consider performance at a regional level [8] to estimate the collective impact of seismic events on buildings and take decisions accordingly. To do this, modifications must be made to the original framework to appropriately model the uncertainties and expected correlations between variables when quantifying the risk of multiple buildings. This led to the formalisation of the regional performance-based earthquake engineering (RPBEE) framework, recently proposed by Heresi and Miranda [8]. The mean annual frequency of exceeding a certain number of damaged buildings can be calculated with Equation (2):

$$\lambda\left(N_{DS} > x\right) = \int_{rup} P\left(N_{DS} > x|rup\right)\left|d\lambda_{rup}\right| \tag{2}$$

where $d\lambda_{\text{rup}}$ is the mean annual frequency of the considered rupture, which is characterised by the hazard of the region, and $P(N_{\text{DS}} > x|\ rup)$ is the probability of exceeding more than x damaged buildings for each considered rupture. Such probability can be estimated using different methods, one being characterising N_{DS} with a binomial distribution. This relies on the assumption that all buildings have an equal probability of being damaged and that the outcome of damage between different structures is independent. As presented in the following sections, these assumptions might incur an oversimplification of the problem that can result in inaccurate estimations of regional risk. An alternative that allows more general cases and complex correlations to be considered between different variables involves Monte Carlo simulation to determine $P(N_{\text{DS}} > x|\ rup)$. This way, the problem is disaggregated by separately sampling each structure's DS from its respective fragility function $P(D > C|IM)$. Then, the total number of buildings that experience damage is counted, and the process is repeated for numerous trials to compute the required statistics.

A fundamental step in this process is estimating the expected level of shaking at each building's geographical location for the considered rupture. This approach shifts hazard characterisation from a scalar value at a single location to a vector representing the IM values across the M building sites: $IM = \{im_1, im_2, \ldots im_n, \ldots, im_M\}$. Since a probabilistic approach is used, IM values are typically considered as random variables characterised by a multivariate lognormal distribution, with the mean values and standard deviations estimated from ground motion models (GMMs), and the corresponding correlation matrix of ground shaking generally referred to as spatial correlation. The justifications for considering the spatial correlation as well as its effects have been widely studied in the past, leading to the development of several mathematical models to estimate it (e.g., in refs. [9–12]).

Regarding fragility estimation, deriving a specific fragility function for every building in the region would require detailed structural information that is usually not available, and would be a highly time-consuming process. As an alternative, a common approach is grouping the structures with similar characteristics and expected similar behaviours into so-called taxonomies (e.g., in refs. [13, 14]). This relates directly to the way in which damage is considered at a regional scale, where the focus is on the overall, rather than individual, performance of buildings. Global displacement-based DSs, such as light damage or collapse, are typically considered, with fragility functions derived for each taxonomy, although recent progress to consider acceleration-based demands in DS definitions and regional loss estimation has been made (e.g., in refs. [15–17]). Different efforts have been conducted to do this, with a notable effort by the Global Earthquake Model (GEM) Foundation, which has created and catalogued fragility (and vulnerability) functions for commonly observed taxonomies worldwide [18].

Applying a single fragility function to all buildings within a taxonomy implies that each building i has the same probability of exceeding a given DS at a particular IM level, im_{n} (i.e., $P_i(D > C|IM = im_n) = P(D > C|IM = im_n)$). However, in a specific earthquake scenario for which the IM level and taxonomy fragility function are known, each building either exceeds the DS or it does not; the notation of probability instead refers to several trials of the same shaking scenario. In regional assessments, it is generally assumed that the exceedance of a DS by one structure is conditionally independent of the damage experienced by others, given the IM level at each location. Nevertheless, some statistical dependence still exists due to spatial correlation of the IM values themselves between sites. For example, the median IM values are typically estimated using the same GMM for a common combination of rupture characteristics; under similar site conditions, inter-event residuals are considered as fully correlated across sites, and an intra-event spatial correlation model is usually used, as studied by Giorgio and Iervolino [19], among others. Recognising that the

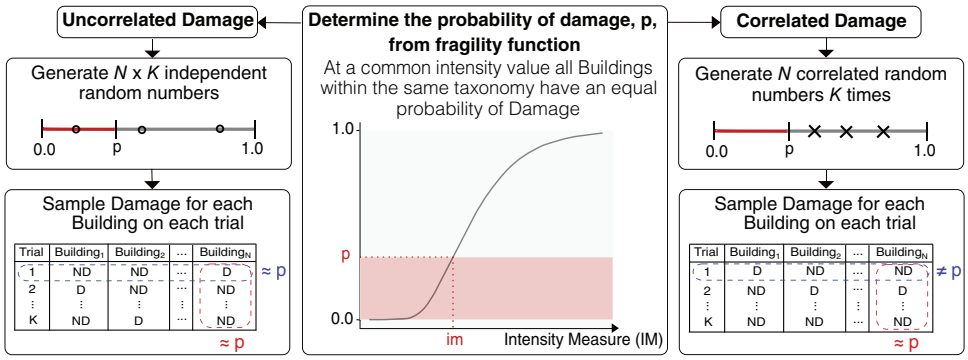

FIGURE 1 | Flowchart for performing Monte Carlo simulation to investigate the impact of correlated and uncorrelated damage (D) (and also no damage [ND]) for a set of buildings within the same taxonomy subjected to a constant level of shaking.

assumption of complete independence of damage is not entirely valid due to the statistical dependencies associated with the experienced IMs, for the sake of linguistic simplicity, this case will be nonetheless referred to as independent or uncorrelated damage.

So, when the performance of several buildings is considered independent, and the ground shaking experienced by each building is constant, $P(D > C|IM = im_n)$ can also be thought of as the percentage of buildings within the taxonomy that surpassed the DS threshold. This is typically done via Monte Carlo simulation from the taxonomy fragility function to simulate a set of buildings that have exceeded DS for a given earthquake scenario, as can be seen in Figure 1, where for a given trial K in uncorrelated damage (i.e., horizontal statistics), the fraction of buildings in a damaged state is equal to the probability p determined from the fragility function. Similarly, for a single building, over several trials 1 through K (i.e., vertical statistics), the fraction of damaged buildings is also equal to the same probability p.

This example is a classical approach to the problem and assumes that during individual trials of a single earthquake scenario, the performance of buildings is independent. However, it is reasonable to assume that structures built in the same region during the same period were likely designed and constructed with a common design code, as well as similar construction practices, resulting in them having either similar strengths and/or deficiencies [20]. A notable example evidencing this dependence occurred in Medellín, Colombia, during the 2010s. Several buildings constructed by the same company and designed by the same structural engineer exhibited significant structural deficiencies. This led to the collapse of a tower of the residential project Space in October 2013 [21], followed by the controlled demolition of the remaining five towers of the same project [22]. Later, two other projects built and designed by the same professionals were also demolished due to significant structural damage [23, 24]. In addition to that, at least two other projects of the same company had to be evacuated due to safety concerns, and structural assessment studies were developed for many others [25]. Studies developed to determine the causes of the deficiencies in the buildings found several contributing factors, such as inadequate structural design and the use of materials with lower mechanical properties than the ones assumed in the design, as well as the inconsistencies between the constructed dimensions of structural elements with respect to those specified in the structural plans [21]. Given that these failures occurred under gravity loads alone, it is highly probable that these structures would have suffered severe damage in the event of an earthquake.

As observed from the previous example, it is logical to expect then that if a single earthquake causes one building to experience a certain level of damage, the same outcome is likely to occur to structures with similar characteristics subjected to similar levels of ground shaking, which will be addressed later. This is why, in regional seismic risk assessment, it is crucial also to consider the potential statistical dependence on the damage of different structures, which is generally represented with what has been defined as *structure-to-structure* damage correlation. This type of correlation is generally either neglected by risk modellers or handled in a very simplified way. Heresi and Miranda [20], among others, have illustrated how it can significantly affect the risk estimated over an entire region [15]. The implications of incorporating this variable into the analysis, compared to the case in which damage is assumed to be independent, are once again presented in Figure 1. Here, the Monte Carlo simulations from the fragility function are no longer independent, meaning that for a given trial K in correlated damage (i.e., horizontal statistics), the fraction of buildings in a damaged state is not equal to the probability p determined from the fragility function but likely much higher or lower. However, for a single building, over several trials 1 through K (i.e., vertical statistics), the fraction of damaged buildings is still equal to the probability p. This is the key difference between considering and not considering the aforementioned *structure-to-structure* damage correlation in regional seismic risk assessment.

This study examines how this structure-to-structure damage correlation may be calculated for residential building typologies typically found in Italy using analytical models. Different methodologies were investigated for different and similar taxonomies (i.e., inter- and intra-structure correlation), and commentary on the benefits and drawbacks of each was explored. A case study in the province of Caserta in Italy was then used to test the methodologies and to demonstrate the impacts that considering and neglecting it can have, especially with respect to the spatial correlation of ground shaking in a regional seismic risk assessment. Calculating the *structure-to-structure* damage correlation from empirical data from past events would generally

be the preferred approach. However, the availability and quality of such data in terms of information on architectural distribution, mechanical properties of the materials, slab type, storey height, and so forth, which are some possible sources of dependence in the damage of different buildings, are not always readily available. Hence, while analytical models might not represent all sources of *structure-to-structure* damage correlation, they still provide the means to account for some of them, offering improved estimates to what is currently available.

2 | Accounting for Structure-to-Structure Damage Correlation in Buildings

2.1 | Background Review

Unlike the spatial correlation of IMs employed in seismic hazard analysis, which has been extensively studied with several mathematical models developed to quantify it, structure damage correlation has received comparatively less attention. In most analyses, this variable is either entirely neglected or treated simplistically by assigning a constant value across all structures (e.g., in refs. [26–28]). Nevertheless, recent efforts have sought to understand this issue better and enhance regional risk models by incorporating more accurate representations of damage correlation.

One of the earliest studies was by Lee and Kiremidjian [29], who investigated the effects of considering the structure-to-structure damage correlation on spatially distributed bridge systems, primarily focusing on transportation networks. Specifically, the damage correlation was estimated for bridges within the same network, assuming an equi-correlated scenario, in which the correlation between the DS experienced by structures a and b, $Corr(DS_a, DS_b)$, was estimated as 1 for $a = b$ (i.e., the structure's DS is perfectly correlated with itself) and ρ for $a \neq b$, with $\rho \in [0,1]$ (i.e., the damage to structure a is correlated to structure b by the same amount that structure c is to structure d). While the correlation was assumed independent of ground motion intensity, it varied with the damage level and was viewed as an optimisation problem. Using least squares adjustment, the marginal probabilities of each bridge's DS were imposed as constraints. A sensitivity analysis revealed that as the correlation increased, the variance in total loss also grew, emphasising the importance of accurately quantifying and incorporating this correlation.

Subsequent approaches expanded on this work; DeBock et al. [30] studied a method for incorporating spatial correlations between EDPs obtained by performing non-linear time history (NLTH) analyses on computational models of buildings for different recordings of the same event in stations located at a certain distance. Later, Kang et al. [31] proposed a model to estimate correlations between EDPs based on the results of incremental dynamic analysis (IDA) performed on multiple structures. These approaches, by capturing statistical dependencies in EDPs, implicitly have the same effects as accounting for structure-to-structure damage correlation; however, they are not directly correlating the probabilities of observing certain DS. Meanwhile, Xiang et al. [32] introduced an analytical model for deriving damage correlation based on structural dynamic properties and spatial separation. This model employed equivalent single-degree-of-freedom (SDOF) systems subjected to consistent and spatially variable white noise.

Heresi and Miranda [20] approached the issue by modelling a structure being in a DS as a Bernoulli trial, where the correlation between two structures could be derived from their marginal probabilities and the joint probability of both experiencing damage under given ground motions. The authors represented the joint distribution with a Gaussian copula, a bivariate normal distribution with a mean vector equal to zero and a given covariance matrix. However, selecting an appropriate correlation factor for the copula remains challenging. To address this in their case study illustration, Heresi and Miranda [20] proposed an equation inversely proportional to the distance between structures and the difference in their construction years. Although this equation was neither tested nor validated but rather based on experience and engineering judgement, it nevertheless illustrated how different values of structure-to-structure correlation could significantly affect regional risk assessment outcomes, especially when collectively dealing with multiple structures and not individual assets as a part of a more holistic decision-making process.

Among the methods mentioned above, the approach proposed by Heresi and Miranda [20] is particularly well-suited for regional seismic risk assessment methodologies. It not only allows the use of fragility functions widely used in the literature, like the ones derived by GEM [18], but also acknowledges that the correlation value should not be uniform across all buildings, given their varying characteristics. Additionally, the challenge of selecting the correlation for the Gaussian copulas can be addressed by developing mathematical models and performing regressions with data from actual historical events or derived from simulated scenarios. With this in mind, an extension of this approach was used in the case study to estimate the damage correlation described herein.

2.2 | Computing Correlation Between Bernoulli Trials

A Bernoulli trial is an experiment whose outcome is random and yields one of only two possible outcomes: success or failure [33], where the probability of success is denoted as p. In the context of seismic events, a building being above or below a certain DS can be visualised as a Bernoulli trial, where a successful outcome corresponds to the structure being above a defined DS, denoted ds, and a failure corresponds to the structure being below it. This probability can be obtained by the fragility function for *Building a* at a given IM value im_n, where $P(DS_a > ds|IM = im_n)$ is denoted simply as p_a.

Therefore, the structure-to-structure damage correlation for two buildings, a and b can be estimated using the equation for the correlation between two Bernoulli trials:

$$\rho_{DS^a,DS^b|im_n,im_m} = \frac{P_{a,b}(DS^a > ds \,\&DS^b > ds\,|im_n, im_m) - P_a\,(DS^a > ds|im_n)\,P_b\,\left(DS^b > ds|im_m\right)}{\sqrt{P_a\,(DS^a > ds|im_n)\,(1 - P_a\,(DS^a > ds|im_n))\,P_b\,(DS^b > ds|im_m)\,(1 - P_b\,(DS^b > ds|im_m))}} \tag{3}$$

For simplicity, the previous equation is denoted from now on as:

$$\rho_{a,b} = \frac{p_{a,b} - p_a p_b}{\sqrt{p_a\,(1 - p_a)\,p_b\,(1 - p_b)}} \tag{4}$$

where p_a and p_b correspond to the marginal probability of buildings a and b experiencing a given DS conditioned on the intensity experienced at their respective locations, im_n and im_m, and $p_{a,b}$ represents the joint probability of both buildings sustaining damage at the intensity experienced by the respective locations. Therefore, the estimated correlation is also indirectly dependent on the intensity values at the building site locations.

Although the marginal probabilities are already known by the fragility curves of the buildings, typically derived for specific taxonomies, sufficient data on the joint probability of damage is often unknown. As a solution, Heresi and Miranda [20] proposed the use of Gaussian copulas as a way of estimating the joint distribution mathematically from the already known marginal probabilities of damage of each building. Alternatively, such distribution could also be estimated analytically from the results of NLTH analyses, as presented in the following section. However, implementing this method requires detailed information to develop non-linear models for all buildings within the studied region, posing a significant challenge.

2.3 | Estimation of Joint and Marginal Probability Distributions

NLTH analysis is a cornerstone methodology in earthquake engineering, enabling the estimation of a building's non-linear response to seismic shaking. While primarily used in risk assessment to analyse single buildings and derive fragility functions, NLTH analyses can be extended to estimate the joint probability of damage between structures. Two widely used methods for NLTH analysis are IDA [34] and multiple stripe analysis (MSA) [35]. IDA performs NLTH analyses with a single set of ground motion records, incrementally scaled to arbitrary IM levels until observing collapse, offering a continuous picture of the evolution of the EDP with respect to IM.

Although IDA has been very useful in PBEE, it has some limitations that must be highlighted. One major issue is the selection of ground motion records for the analysis, since different studies have shown that the NLTH analysis results can be significantly affected by the chosen set of records (e.g., in ref. [36]). Additionally, there may be some bias in the results of analyses when records are significantly scaled [37]. The extent of this bias depends on the selected IM for the analysis, where Dávalos and Miranda [38], for instance, showed that $Sa(T_1)$ is an IM significantly prone to bias. Although this issue can be avoided by using alternative IMs or simply inspecting the results to ensure no bias, as shown by O'Reilly [39] and Aristeidou and O'Reilly [40], for example, it is generally preferred to use MSA [34] in such cases, which shares the same principle as IDA, with the difference that the records are selected to be hazard-consistent at each individual IM level (stripe), limiting the scaling factor required in many cases. It is important to know, however, that with MSA it is not possible to deduce a continuous picture of the EDP's evolution with respect to IM—as in the case of IDA—since the data cannot be interpolated given that a different ground motion record set is used for each IM stripe.

Following the same methodology used to estimate the probability of a particular building exceeding a certain DS for a given IM, which in the context of this study corresponds to the marginal probability of damage, it is possible to estimate the joint probability of damage of two buildings from the results of NLTH analyses, denoted $p_{a,b}$. If the same set of ground motion records is used for all models, the probability of two buildings exceeding a DS can be estimated by counting the records for which the corresponding limit EDP was exceeded for both buildings simultaneously for both records and dividing by the total number of records, as follows:

$$p_{a,b} = \frac{z_{a,b}}{n} \tag{5}$$

where $z_{a,b}$ is the number of observations in which both buildings a and b result in a given DS and n is the total number of records used for the analysis. The value of $z_{a,b}$ can be estimated either from the results of MSA, as presented in Figure 2, or from the results of IDA, as presented in Figure 3.

Given the limitations of IDA discussed earlier, the ideal approach would involve using the results of MSA on all buildings. However, as previously mentioned, MSA requires a different set of records for each stripe, making it near impossible to interpolate the EDP results for IM values other than those corresponding to the one for which the records were selected. This limitation means that MSA can only be used in a hypothetical scenario where all buildings experience a constant level of ground motion shaking (i.e., $im_n = im_m$), which is unlikely, with an IM corresponding to that of a particular stripe, where the same IM is assumed to be used for both buildings, as illustrated in Figure 2.

In reality, where each building experiences a different IM level, a viable alternative is to use the results obtained by performing an IDA on the buildings. This involves modelling the expected IM level at each site and then interpolating the EDP values for each building at the corresponding IM level for each record. Once this is done, the joint probability can be estimated from Equation (5) and as illustrated in Figure 3 for the case of $im_{\mathrm{n}} \neq im_{\mathrm{m}}$. The marginal probabilities used to estimate the correlation from Equation (4) are calculated from the results of either MSA

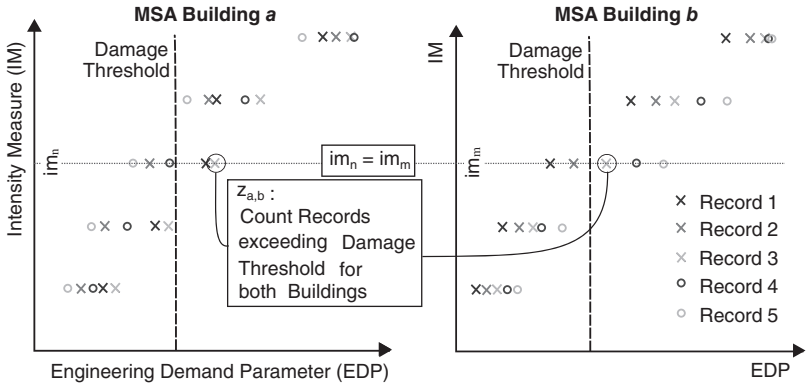

FIGURE 2 | Estimation of joint probability distribution from MSA results. MSA, multiple stripe analysis.

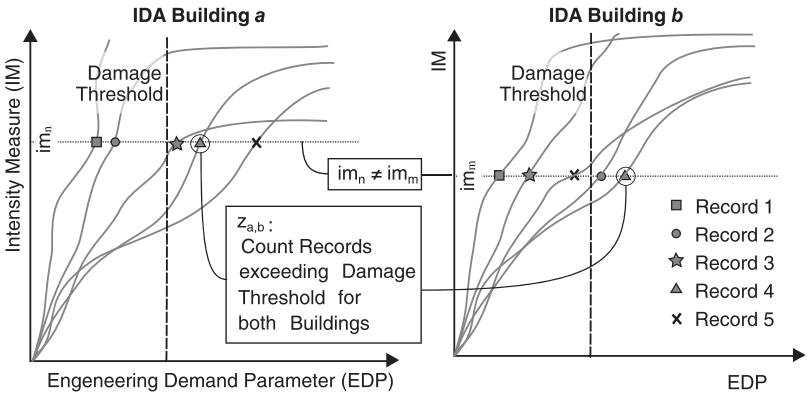

FIGURE 3 | Estimation of joint probability distribution from IDA results. IDA, incremental dynamic analyses.

or IDA as follows:

$$p_a = \frac{z_a}{n} \tag{6}$$

$$p_b = \frac{z_b}{n} \tag{7}$$

where z is the number of observations of a given DS and n is the number of ground motions. The correlation can then be calculated from Equation (4) using the joint probability obtained in Equation (5) and the marginal values obtained from Equations (6) and (7).

One of the advantages of estimating the damage correlation with this method is that it accounts for the dependence of correlation on the considered DS, as structural responses vary with the level of non-linearity experienced. This aspect is incorporated into the methodology through the calculation of joint and marginal probabilities, as defined by Equations (5), (6), and (7), that yield different results based on the considered DS. As a result, the estimated correlation inherently depends on the considered DS in each structure investigated. In addition to that, with the results of IDA, it may also be possible to estimate correlations across different DS between structures (i.e., collapse at structure *a* with light damage at structure *b*), although this aspect was not addressed here and is noted as a potential future development.

It is important to note that estimating joint probabilities from MSA is limited not only by the requirement that the IM value must be constant across all buildings (Figure 2), but also by the need to use the same type of IM (e.g., PGA) for the assessment of all buildings. However, structural response can be characterised more efficiently by using IMs better linked with their specific dynamic characteristics like $Sa(T_1)$. The use of next-generation IMs like $Sa_{avg}(T^*)$ has shown more efficient fragility estimations [41] and could pose a solution to the inefficiency issue, and the final period range for which $Sa_{avg}(T^*)$ is computed captures the expected variations in the period as all buildings start to behave non-linearly. There are some special considerations that must be made if $Sa_{avg}(T^*)$ is selected as the IM for the analysis. Traditional seismic hazard assessments have been conducted without the inclusion of $Sa_{avg}(T^*)$. However, recent advancements in GMM developments have made its inclusion feasible (e.g., in refs. [38], [42], [43]) and on ways of estimating the spatial correlation for $Sa_{avg}(T^*)$, as well as methods for estimating the spatial correlation like the indirect approach proposed by Heresi and Miranda [44]. Similar challenges are encountered when dealing with the fragility functions, since those found in the literature are rarely estimated in terms of $Sa_{avg}(T^*)$; therefore, it would be necessary to convert the IM of the fragility function with methodologies such as the one proposed by Suzuki and Iervolino [45]. However, if the structure-to-structure correlation is estimated with IDA (which was the method ultimately used in this study), a common set of ground motions can generally be used for all structures. To develop correlation models that span different IMs for different structures, the IM value of each ground motion used in the analysis can be computed for each structure. Then, when ground motion fields are calculated using spatial cross-correlation

models, resulting in a simulated intensity at the location of each building in terms of its respective IM, a correlation model that has been developed for the two different IMs can be used.

Finally, it must be noted that this method has a high computational cost, as it requires running several records at various IM levels on all buildings of the region under assessment. It is possible, however, to explore the applicability in this specific context of different approaches commonly used to simplify the process of generating fragility curves. One of the most common approaches [18] is by using equivalent SDOF oscillators with properties derived from the pushover curve of the buildings, which approximates the behaviour of a multiple degree of freedom building assuming regular response and first-mode dominance and displacement-based DSs. This methodology was employed by Martins and Silva [18] and also by Nafeh et al. [46] as a simplified method for assessing infilled structures, for example, and will be discussed below.

2.4 | Implementing Structure-to-Structure Correlation in Regional Damage Assessment

Once the correlation between Bernoulli trials has been calculated from Equation (4) for each pair of buildings in the portfolio, it is possible to utilise this and estimate damage scenarios due to any particular earthquake scenario using Monte Carlo simulation, whilst also accounting for structure-to-structure damage correlations. The general procedure follows the method proposed by Emrich and Piedmonte [47] to generate correlated binary random variables, which considers that the joint distribution of the data can be approximated from a multivariate normal distribution. The steps to follow are:

1. For the considered rupture, simulate the value of the IM at the location of each building in the portfolio using an appropriate GMM and spatial correlation model for the considered region.
2. Using Equation (4), calculate the value of ρ_{ab} for each pair of buildings for their respective IM value estimated in the previous step.
3. For each pair of buildings, a and b, find the structure-to-structure correlation value of the multivariate normal distribution, δ_{ab}, by solving Equation (8):

$$\Phi\left[\Phi^{-1}(p_a), \Phi^{-1}(p_b), \delta_{ab}\right] = \rho_{ab}\sqrt{p_a(1-p_a)\,p_b(1-p_b)} + p_a p_b \tag{8}$$

   where this is simply a reworking of Equation (4) with the assumption that the joint probability p_{ab} can be represented using a Gaussian copula function $\Phi[\cdot]$ with inherent correlation δ_{ab}, as per Heresi and Miranda [20].
4. Given that N is the total number of buildings considered in the assessment, sample a vector of correlated random variables $X = \{x_1, x_a, x_b, \ldots, x_N\}$ with a mean vector equal to zero $\mu_X = \{0, \ldots 0\}$ and covariance Σ_X, where $\Sigma_X(a,b) = 1$ for $a = b$ and $\Sigma_X(a,b) = \delta_{ab}$ for $a \neq b$.
5. From vector X, obtain a vector of correlated uniformly distributed variables $U = \{u_1, u_a, u_b, \ldots, u_N\}$ such that:

$$u_a = \Phi(x_a) \tag{9}$$

6. From this vector of U values, estimate the DS of every building by taking the probability of exceedance of the considered DS from every building's respective fragility function conditioned on the IM estimated in *Step 1*, $P_a(\mathrm{DS}^a > \mathrm{ds}|im_n)$. The structure is simulated as being in DS if $u_a < P_a(\mathrm{DS}^a > \mathrm{ds}|im_n)$, or otherwise undamaged.

The steps above are equivalent to implementing the approach illustrated in Figure 1, where the grey cross marks are simulated as correlation trials to estimate damage scenarios. If the correlations had been ignored (i.e., $\Sigma_X(a,b) = 0$), then this is akin to simulating the grey dots in the same figure. It is important to consider that this procedure, as it is outlined here, considers just one DS. Including additional DSs would increase the complexity of the problem (e.g., cross-DS correlations) and would require further considerations but is nonetheless feasible. Having simulated the DS of each building, it is possible to estimate the total number of buildings in a given DS by simply counting them in a single trial, allowing the probability of observing more than x damaged buildings for the considered rupture, $P(N_{\mathrm{DS}} > x|\ rup)$, to be estimated. If the procedure is repeated for other possible ruptures in the area, a regional damage estimation can be obtained by applying Equation (2).

3 | Definition of Case Study

A regional seismic risk assessment of mid-rise residential reinforced concrete (RC) frame structures was conducted to study the effects of structure-to-structure damage correlation in a real-world setting. A portfolio of buildings was generated with the Built Environment Data (BED)'s SimDesign service (https://simdesign.builtenvdata.eu/) [48], which allows non-linear models of simulated buildings representative of specific eras in construction practice to be obtained. This tool simulates building characteristics using Monte Carlo simulation, estimating structural features based on their observed regional proportions. This approach offers a practical alternative for applying the proposed method to calculate structure-to-structure damage correlation, since developing non-linear models for all buildings of a specific taxonomy in a region is highly time-consuming and, in many cases, unfeasible due to the lack of detailed information required to construct such models. However, with such a tool available, this could be simulated based on existing knowledge to produce representative buildings from each construction era with relative ease.

To ensure the simulated buildings reflect realistic conditions and hence better characterise the relative impact of structure-to-structure correlation on regional assessments, their characteristics were estimated based on real-world data from a study by Corlito and De Matteis [49], in which detailed structural properties of RC buildings across eight municipalities were collected for the Caserta province in Italy. It was decided to focus on three municipalities: Castello del Matese, Gioia Sannitica, and Piedimonte Matese, which share a similar high seismic hazard

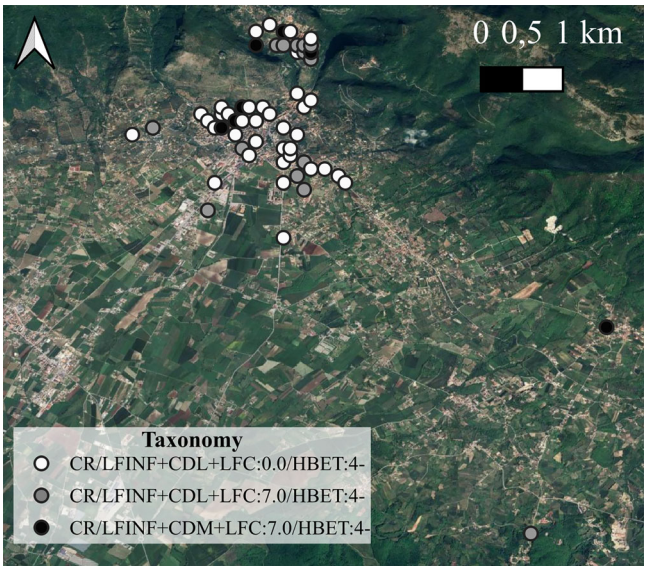

FIGURE 4 | Assumed spatial distribution of the assets studied within the three municipalities.

classification according to the Italian building code, *Norme tecniche per le costruzioni* (NTC18) [50]. The number and locations of buildings in the analysis were derived from an accurate exposure model, reflecting the actual portfolio of buildings of the selected typologies in the studied municipalities, as described below.

3.1 | Exposure Model

The exposure model adopted was the one used in the European seismic risk model (ESMR20) [51]. It divides the buildings into residential, commercial and industrial use classes and categorises them according to the GEM Building Taxonomy v3.1 [52]. For this case study, only residential buildings with more than four storeys were considered, including all code levels and design lateral force coefficients found in the area. A total of 62 buildings were found to be in the studied municipalities, distributed into the following taxonomies:

- CR/LFINF + CDL + LFC:0.0/HBET:4-: Low code RC infilled frames with more than four storeys designed for a load factor of $\beta = 0\%$ (41 buildings).
- CR/LFINF + CDL + LFC:7.0/HBET:4-: Low code RC infilled frames with more than four storeys designed for a load factor of $\beta = 7.0\%$ (15 buildings).
- CR/LFINF + CDM + LFC:7.0/HBET:4-: Moderate code RC infilled frames with more than four storeys designed for a load factor of $\beta = 7.0\%$ (6 buildings).

Since the exposure model aggregates all buildings in each municipality to a single point, spatial disaggregation was performed using GEM's spatial disaggregation repository [53]. The data on the distribution of the population used for the analysis was obtained from the WorldPop data of Italy for the year 2020, with a resolution of 100 m [54]. The spatially disaggregated location of the assets adopted for this study is presented in Figure 4. While these do not necessarily correspond to the actual locations of these typologies, it is not envisaged to have any impact on the overall conclusions of the work; the focus of this study is to examine the impacts of structure-to-structure correlation on a case study evaluation of a realistic area exposed to seismic hazard.

The categorisation of the codes into low or moderate and the definition of the lateral load coefficient, β, follow the generalised definition presented in Crowley et al. [55]. It was defined based on common standards of a particular generation of seismic design norms. CDL codes, for instance, consist of the first generation of design codes in which material-specific standards and allowable stress design were performed. On the other hand, CDM codes are considered second-generation codes that included the first concepts of capacity design and some details to improve ductility. The value of β represents the percentage of the mass of the building that is being applied as a lateral force for the design of the building and is not only dependent on the hazard of the site but also on specific code requirements like behaviour or importance factors. Since the category of the code is related to the generation of the code in Europe, it is possible to find that in a region there are more than one code classified into a particular category. In Italy, for example, three different norms were classified as CDL, the ones from 1915, 1935, and 1984 [55]. It is possible then that the required value of β changed from one CDL code to another CDL code, so it is a variable that introduces an additional variation on the expected response of the buildings. While β is undoubtedly an uncertain parameter with several contributing factors, it was adopted here to maintain some integration with taxonomy-based studies that use the CDL, CDM, and other such definitions in the literature.

3.2 | Simulated Design and Numerical Modelling

Since 62 buildings were found across the three municipalities from the exposure model, a similar-sized portfolio of buildings and numerical models was simulated with the BED's SimDesign service following structural attributes obtained from Corlito and De Matteis [49]. Each building was then designed using the equivalent lateral force method, following European standards depending on the desired level of the design code and using the respective value of β. The resulting numerical models were then generated by the tool in OpenSeesPy [56], allowing NLTH analyses to be performed and fragility functions to be developed, as well as the structure-to-structure damage correlation to be estimated with the methodology described in Section 2. The numerical models were developed with each building being modelled with elastic elements for beams and columns, with their stiffness being modified according to Zareian and Medina [57]. To model non-linearity, a lumped plasticity approach was used, with the location of *zeroLength* elements at both ends of the elements simulating the moment-rotation response of plastic hinges. The yield moment and rotation capacity were estimated as proposed by Panagiotakos and Fardis [58] and Eurocode 8 – Part 3 [59]. The other parameters were estimated from Haselton et al. [60] and ASCE/SEI-41/17 [61]. The bond slip factor was considered in the computation of the plastic rotation capacity. Further details are outlined in Ozsarac et al. [48].

Additional springs were located to account for potential shear failure in the columns for the cases in which capacity design

TABLE 1 | Hazard analysis results with the computed $Sa_{avg}(T^*)$ values for different return periods.

Return period [years]	22	42	72	140	224	475	975	2475	4975	9975
PoE in 50 years	0.897	0.696	0.501	0.300	0.200	0.100	0.050	0.020	0.010	0.005
$Sa_{avg}(T^*)$ [g]	0.021	0.044	0.072	0.123	0.166	0.268	0.383	0.577	0.746	0.945

principles were not considered during the design of the building. For the hinge material, the three-point limit curve proposed by Elwood and Moehle [62] and Elwood [63] was adopted. The shear strength was estimated from ASCE/SEI-41/17 [61] with the strength degradation model proposed by Sezen and Moehle [64]. Beam-column joints were modelled as *zeroLength* elements, considering the joint flexibility in the rotational degrees of freedom, using inelastic, elastic or rigid materials depending on the joint type. Inelastic joints were modelled as a *Hysteretic* uniaxial material with parameters obtained with expressions specified by O'Reilly [65] and O'Reilly and Sullivan [66].

Pushover analyses and modal characteristics were performed to calculate the properties of the equivalent non-linear SDOF oscillators. The buildings were distributed geographically across the area, assigning them a random location from the spatially disaggregated exposure model.

3.3 | Seismic Hazard

Seismic hazard was quantified via PSHA at the site location corresponding to the mean coordinates of all the buildings considered in the region using the 2013 European Seismic Hazard Model (ESHM13) [67]. This was a simplifying assumption to avoid conducting building-specific PSHA (and subsequent ground motion record selection) that would have resulted in a drastically increased computational cost. The GMM considered was the one developed by Boore et al. [68], assuming a firm soil with $V_{s,30} = 480$ m/s, and the spatial correlation model by Jayaram and Baker [11] was adopted. The IM selected for the analysis was the average spectral acceleration over a period range, $Sa_{avg}(T^*)$, which has been demonstrated in several past studies to offer many benefits in terms of efficiency and sufficiency (e.g., in refs. [36], [39], [44], [69–71]). The period of the range for the analysis was defined based on the limits proposed by Eads et al. [41], which consists of a lower limit of $0.2T^*$ and an upper limit of $3.0T^*$. The value of T^* was calculated as presented in Equation (10):

$$T^* = \frac{1}{N}\sum_{b=1}^{N}\sqrt{T_{1X,b}T_{1Y,b}} \tag{10}$$

where N is the total number of buildings and T_{1X} and T_{1Y} are fundamental periods of the building b in the two orthogonal directions. For the portfolio considered, T^* was computed as 0.605 s, meaning the selected period range was 0.12 to 1.82 s. The $Sa_{avg}(T^*)$ intensity levels for different return periods and probability of exceedance (PoE) in 50 years are presented in Table 1. For each return period, 40 ground motion records were selected following the conditional spectrum method described by Lin et al. [72] using the Djura Record Selector (https://apps.djura.it/login) to give a ground motion suite that was hazard consistent with the $Sa(T)$ values at different vibration periods.

3.4 | Fragility Estimation

Regarding fragility functions, different approaches can be considered to identify and implement them in regional studies. On one hand, structure-specific fragilities can be derived from a fully defined model of a particular structure, capturing all geometric, material, and structural details. When performing regional analysis, developing structure-specific fragility functions for each building renders this approach cumbersome and unscalable, and has led to a more pragmatic approach of using taxonomy-based fragilities [73]. Taxonomy-based fragilities are intended to represent the response of a population of buildings sharing common characteristics (e.g., structural system, number of storeys, construction era). Unlike structure-specific fragilities, where the primary uncertainty is intra-building, taxonomy-based fragility functions have an added uncertainty associated with the inter-building variability for a given taxonomy class. While a taxonomy-based approach would commonly be used for case studies like the one presented here, it was decided to work with structure-specific fragilities. This was because the number of buildings in the case study region was still feasible to analyse individually, and also because it would allow the issue of structure-to-structure damage correlation to be better isolated and examined without the interference of inter-building variability being present initially. The approach adopted herein was to better understand the issue on a structure-specific scale and quantify its relative impact (if any). The findings will be extended in future work to better align with regional studies adopting a taxonomy-based fragility function approach where inter-building variability is accounted for. In this respect, the use of equivalent SDOFs to characterise correlations between individual structures could be investigated to characterise and assess entire classes (e.g., as discussed in ref. [74] when extending to regional assessments).

Structure-specific fragilities were derived for each of the buildings from the results of the NLTH analyses, which were performed in any case to allow the *structure-to-structure* damage correlation to be estimated, as described in Section 2. Two types of analyses were conducted: first, MSA was performed on the full 3D models of the structures; and second, IDA was performed on equivalent SDOF oscillators. Using MSA represents a more thorough approach considering full model behaviour and hazard-consistent ground motions; however, it comes at a great computational cost in addition to presenting difficulties in quantifying correlations between buildings experiencing differing IM levels, as discussed previously. IDA was conducted using the single set of ground motion records selected for an intensity of $Sa_{avg}(T)$ equal to

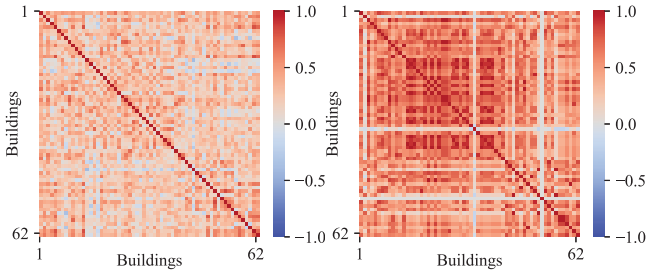

FIGURE 5 | Correlation matrices calculated for $Sa_{avg}(T) = 0.268$ g and PDR > 1%, using results from MSA (left) and IDA on SDOF (right). IDA, incremental dynamic analyses; MSA, multiple stripe analysis; SDOF, single-degree-of-freedom.

0.268 g. By adopting IDA, the effect of using equivalent SDOF oscillators to estimate correlations compared to the results of the full 3D model and hazard-consistent MSA was studied.

The process of performing IDAs on the equivalent SDOF systems involves several steps. First, a static pushover curve is performed in each building direction and converted to an equivalent SDOF system as described by O'Reilly and Shahnazaryan [16]. During the linearisation process, priority was given to preserving the maximum strength of the building rather than matching the areas beneath the original and linearised curves, as the maximum strength was deemed a more representative parameter of the building's mechanical behaviour. Next, the NLTH analyses were performed to generate the IDA curves for each building. Subsequently, the results were transformed back to represent the original MDOF building.

Given the inherent limitations of IDA previously discussed, the fragility functions derived from the results of MSA were preferred to estimate damage in the case study. The maximum likelihood method was used to fit a lognormal distribution to the results obtained from the MSA. Two different DS were considered: DS_1, *light damage*, defined as the case in which the maximum peak storey drift (PSD) ratio is larger than 1.0%; and DS_2, *collapse*, defined as the case in which the maximum PSD ratio is larger than 8.0%.

3.5 | Quantifying Structure-to-Structure Damage Correlation

Structure-to-structure damage correlation was calculated using Equation (4) based on the results of MSA. The marginal probabilities were obtained through linear interpolation of the discrete data computed with Equations (6) and (7), whereas the joint distribution $z_{a,b}$ was calculated using Equation (5) (Figure 2), acknowledging the limitation that this method only allows damage correlation to be estimated under constant shaking cases. On the other hand, the results of IDA on the SDOF oscillators were used to compute $z_{a,b}$, allowing for the consideration of different intensity levels at the building locations, as shown in Figure 3.

An example correlation matrix calculated using both approaches is presented in Figure 5. It assumes the same intensity of shaking for all buildings to allow MSA-based correlations to be computed and significant differences to be observed. In general, the IDA on SDOFs approach tends to result in notably higher correlations; however, the impact of this in actual damage estimations is further explored in the following sections. It is important to note that some negative values appear in the estimations, primarily due to the limited number of records causing damage to both structures. While such negative values are not physically meaningful in this context, they occur only in specific cases and remain close to zero, so no special adjustments were made. Additionally, the numbering of the buildings was randomly assigned, so no distinct pattern should be expected in the results illustrated other than the diagonal values being equal to unity.

It is important to acknowledge that variations on the results presented in Figure 5 obtained using the IDA on SDOF may arise due to the selected suite of ground motion records. This is, as previously stated, a general limitation of IDA since a single set is typically used and overlooks site-specific hazard features that could influence fragility function development. However, it has been shown that this impact is diminished when $Sa_{avg}(T^*)$ is used for the analysis [36], as was done here. Furthermore, there may be some uncertainty in the estimation of the fragility function's lognormal distribution parameters (i.e., median, dispersion) due to modelling choices and the variability of the results from the specific set of records used to fit them that could ultimately impact the fitted distribution, its classification of DS, and ultimately the computed value of the correlation. To have a general idea of the magnitude in the estimations of uncertainty, the coefficient of variance (COV) of the fitted parameters for Building 15 was estimated, using the parametric resampling method with 1000 realisations and generating 40 samples for each intensity level. It was determined that for DS_1 the fitted parameters have a COV of 4.5% for the mean and 14.6% for the standard deviation, and for DS_2 the obtained values are 6.5% and 16.8%, respectively. The impact of this uncertainty in the estimation of the correlation was therefore not deemed critical but should be studied in future developments of this work.

4 | Analysis for Different Shaking Cases

To evaluate the impacts and applicability of the correlation models previously described, a case study region was examined for different cases to estimate the number of damaged buildings. This included evaluating the impact of structure-to-structure correlation, methods to estimate it and its relative impact (if any) with respect to the more well-known spatial correlation of ground shaking. Depending on the case under evaluation, two DSs were considered: *light damage* (DS_1) and *collapse* (DS_2). A summary of the different combinations is given in Table 2 and explained as follows:

- Case 1: Constant shaking cases were considered to utilise the results of MSA on a full 3D model of the building and compare it with the results of IDA on an equivalent SDOF oscillator. For this purpose, a constant shaking case was employed, with all structures subjected to $Sa_{avg}(T) = 0.268$ g. This hypothetical case assumes that all buildings were located on the exact same site, allowing the IM value to be constant for each building but also isolating the effects of damage correlation from spatial correlation. The selected intensity corresponds to one of the

TABLE 2 | Description of the considered shaking cases for damage estimation of the case study region.

Case	IM value	Damage state	Subcase	Spatial correlation, ρ_{sp}	Damage correlation, ρ_{dm}
1	Constant, with $Sa_{avg}(T)$ equal to 0.268 g	DS_1: PSD larger than 1.0% (light damage)	1.1	—	Not considered
			1.2	—	Considered, from MSA
			1.3	—	Considered, from IDA
2	Constant, with $Sa_{avg}(T)$ equal to 0.746g	DS_2: PSD larger than 8.0% (collapse)	2.1	—	Not Considered
			2.2	—	Considered, from MSA
			2.3	—	Considered, from IDA
3	Calculated based on an earthquake rupture scenario	DS_1: PSD larger than 1.0% (light damage)	3.1	Not considered	Not Considered
			3.2	Considered	Not Considered
			3.3	Not considered	Considered, from IDA
			3.4	Considered	Considered, from IDA

Abbreviations: IDA, incremental dynamic analyses; MSA, multiple stripe analysis; PSD, peak storey drift.

intensity levels for which records were selected to perform MSA, for which the same records with the same scale factors were also used for IDA. DS_1 was considered for this case. Different cases of structure-to-structure damage correlation, ρ_{dm}, were also used from both the MSA- and IDA-based approaches.

- Case 2: Like Case 1, a second hypothetical shaking case was analysed, using one of the highest intensities from the selected records for MSA, with $Sa_{avg}(T) = 0.746$ g, and the collapse DS_2 was considered. Despite being a rather high intensity, it served to investigate the impact that potential bias due to excessive scaling of the records might have on the estimation of the damage correlation when using IDA.
- Case 3: Lastly, a single earthquake rupture scenario was considered to observe the impacts using a more realistic seismic shaking situation and make relative comparisons of the impacts of damage correlation with respect to realistic values of spatial correlation when estimating the number of damaged buildings. DS_1 was considered again for this scenario.

For Cases 1 and 2, 100,000 trials of Monte Carlo simulation were performed, whereas 5000 were considered for Case 3.

4.1 | Case 1: Light Damage at a Constant Shaking of $Sa_{avg}(T) = 0.268$ g

Here, the total number of damaged buildings was estimated using Monte Carlo simulation, accounting for the damage correlation matrix calculated based on the results from the full 3D model. These were compared to the estimation obtained using equivalent SDOF oscillators. The shaking intensity was 0.268 g for all buildings, meaning the records used for calculating the damage correlation matrix with both MSA and IDA were identical. As such, differences in the results can only arise from the analysis method (i.e., equivalent SDOF oscillators). The mean, median and standard deviation from all realisations are presented in Table 3. Although the mean number of damaged buildings is similar across all three cases (approximately 35 buildings), the median varies slightly. The most notable difference is seen in the standard deviation, which increases from 3.7 for Case 1.1 to 20.4 for Case 1.3, affecting the overall shape of the probability distribution, as observed in Figure 6.

TABLE 3 | Statistics on the total number of damaged buildings in DS_1 for cases considered in Case 1.

Statistic	Case 1.1: No correlation	Case 1.2: Correlation from MSA	Case 1.3: Correlation from IDA
Mean	35.1	35.0	35.0
Median	35.0	36.0	38.0
Standard deviation	3.7	15.0	20.4

Abbreviations: IDA, incremental dynamic analyses; MSA, multiple stripe analysis.

This illustrates that considering structure-to-structure damage correlation doesn't impact the estimated mean or median number of damaged buildings, but rather the tails of the distribution through the standard deviation. This increases the probabilities of observing a large number of damaged buildings in a given shaking scenario, which, in the context of regional seismic risk assessment, might be a very pertinent decision variable for the local authorities. To explore how the probabilities of observing a large number of damaged buildings (i.e., a number above the mean value) differ in each case, Figure 7 illustrates this exceedance plot, and Table 4 tabulates it for several thresholds. Considerable differences can be observed between the results obtained by neglecting the structure-to-structure damage correlation and those calculated using either of the two methods employed. For example, the probability of having more than 45 damaged buildings is 39.8% for Case 1.3 and 29.2% for Case 1.2, but only 0.2% for Case 1.1 that ignored any damage correlation. This highlights its importance when evaluating highly impacting scenarios of large numbers of damaged buildings in a region.

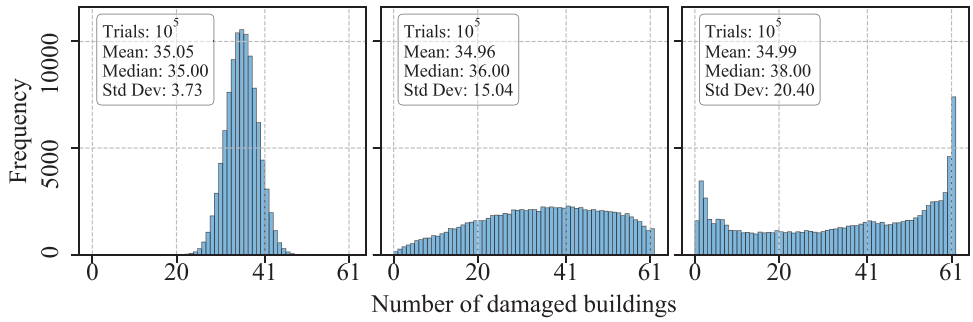

FIGURE 6 | Histograms of the total number of damaged buildings evaluated for Case 1.1 (left), Case 1.2 (centre) and Case 1.3 (right), as well as the estimated statistics.

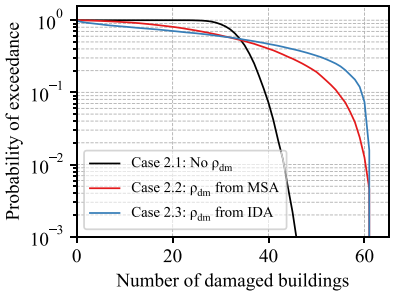

FIGURE 7 | Illustration of the probability of exceeding a given number of damaged buildings in DS_1 for cases considered in Case 1.

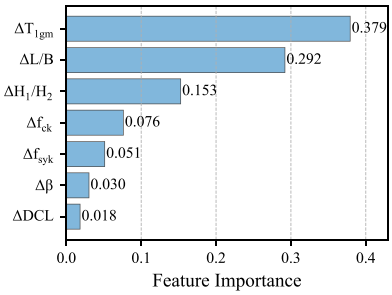

FIGURE 8 | Feature importance from the random forest regression model trained on the absolute differences in structural characteristics between building pairs for correlation estimated with MSA for Case 1. MSA, multiple stripe analysis.

TABLE 4 | Example scenarios of exceedance probabilities for a given number of damaged buildings in DS_1 for Case 1.

Number of damaged buildings	Case 1.1: No correlation	Case 1.2: Correlation from MSA	Case 1.3: Correlation from IDA
30	89.0%	61.6%	60.2%
35	45.5%	51.1%	54.0%
40	7.0%	40.0%	47.2%
45	0.2%	29.2%	39.8%

Abbreviations: IDA, incremental dynamic analyses; MSA, multiple stripe analysis.

When comparing the results from Case 1.2 and Case 1.3, which evaluate the comparison of MSA- and IDA-based estimates, the difference increases as the number of damaged buildings rises until the curves saturate due to the fact that it approached the maximum number of buildings in the portfolio, which was previously noted as 62. This illustrates how using equivalent SDOF oscillators to calculate the structure-to-structure damage correlation results in a slight overestimation of the correlation and subsequently the total number of damaged buildings. However, it still offers a more accurate estimate compared to completely ignoring this correlation, as in Case 1.1, as is usually done due to the lack of direct estimation methods.

To evaluate the influence of different structural characteristics on the damage correlation estimated from the results of MSA, a data-driven analysis was conducted using a random forest regression model. For each building pair, the absolute difference in their structural features was computed and used as input to predict the value of the correlation. The variables considered for the analysis were the geometric mean of the fundamental period in both directions, $T_{1,gm}$; planar aspect ratio, L/B; the soft storey ratio of first storey, H_1/H_2 (calculated as the height of the first storey over the height of the rest of the storeys); the characteristic compressive strength of concrete, f_{ck}; the yield strength of the reinforcement, f_{syk}; the lateral load coefficient, β; and the level of the design code (LDC). The trained model provided feature importance scores, which quantify the relative contribution of each characteristic to explaining variability in *structure-to-structure* damage correlation. The characteristics with the higher feature importance are those that strongly influence the value of the damage correlation. The obtained results are presented in Figure 8.

It can be noted that the variable with the highest contribution is the absolute difference between the geometric means of the fundamental periods of the structures, followed by the difference in the planar aspect ratios and the soft storey ratio. On the other hand, there is very little contribution from the absolute difference between the value of β and the design code level. This is probably since the observed values of β are always relatively low, indicating that, in most cases, the design of the elements was controlled by vertical loads. Regarding the design code level, it has been shown that there tends to be not a significant difference in the response of CDM structures when compared to the ones of CDL structures for values of β below 0.10 [48], which explains the low impact of the difference in design code. It should be expected, however, that in cases with a more significant variability in the values of β

TABLE 5 | Statistics on the total number of damaged buildings in DS_2 for cases considered in Case 2.

Statistic	Case 2.1: No correlation	Case 2.2: Correlation from MSA	Case 2.3: Correlation from IDA
Mean	27.9	27.8	27.8
Median	28.0	28.0	28.0
Standard deviation	3.5	12.9	19.6

Abbreviations: IDA, incremental dynamic analyses; MSA, multiple stripe analysis.

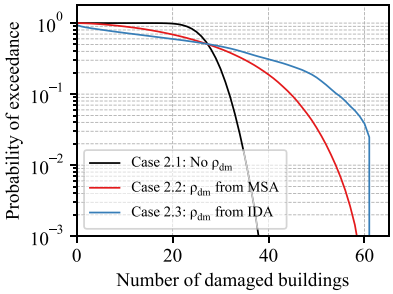

FIGURE 9 | Illustration of the probability of exceeding a given number of damaged buildings in DS_1 for cases considered in Case 2.

and including CDH structures, these two variables would have a higher impact.

4.2 | Case 2: Collapse at a Constant Value of $Sa_{avg}(T) = 0.746$ g

This second case was like Case 1 but instead analysed a higher DS of collapse. A stronger level of uniform shaking was considered with $Sa_{avg}(T) = 0.746$ g. This case was investigated, as it would also reveal potential biases in damage estimation arising from the excessive scaling of records associated with the IDA-based calculation of structure-to-structure damage correlation, which necessitated significant scaling factors as high as 34.5. The total number of damaged buildings obtained from the IDA-based equivalent SDOFs were again compared to those estimated using MSA on full 3D models. The mean, median and standard deviation from all realisations are presented in Table 5. As with Case 1, the mean number of damaged buildings is consistent across all cases, approximately 27.8 buildings, and there is no variation in the median (28 buildings). However, significant differences are observed in the standard deviations, which increase from 3.5 in Case 2.1 to 12.9 in Case 2.2 and 19.6 in Case 2.3, again highlighting the impact of correlations on damage estimation.

Again, the impact of correlation on the probability of exceeding a certain number of damaged buildings is shown in Figure 9 and tabulated for different scenarios in Table 6, where there is a significant difference in the results of considering and neglecting the structure-to-structure correlation. When comparing the results in Figure 9 with those in Figure 7, it can be observed that the

TABLE 6 | Example scenarios of exceedance probabilities for a given number of damaged buildings in DS_2 for Case 2.

Number of damaged buildings	Case 2.1: No correlation	Case 2.2: Correlation from MSA	Case 2.3: Correlation from IDA
25	89.0%	56.4%	53.7%
30	22.5%	43.4%	47.0%
35	1.4%	30.6%	38.8%
40	0.01%	19.1%	31.1%

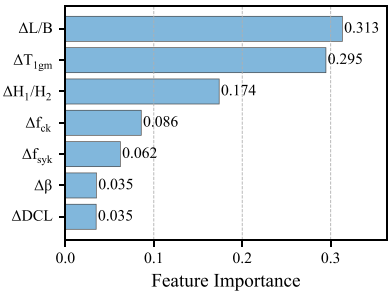

FIGURE 10 | Feature importance from the random forest regression model trained on the absolute differences in structural characteristics between building pairs for correlation estimated with MSA for Case 2. MSA, multiple stripe analysis.

difference between the cases that use MSA and the cases that use IDA on equivalent SDOF is more pronounced in this case. For example, when looking at the example scenario of exceeding more than 40 damaged buildings, as presented in Table 6, a significant difference is observed. The results obtained for Case 2.3 (31.1%) are notably higher than those for Case 2.2 (19.1%). It is still, however, a better approximation to the result than completely neglecting the correlation, for which the probability of exceeding a total number of 40 damaged buildings is nearly negligible (<0.01%).

As for Case 1, the influence of the absolute difference between different parameters of the buildings was estimated using a random forest regression model, and the results for Case 2 are presented in Figure 10. Here, the considered DS is collapse, and there is a lesser importance from the differences in the fundamental periods of vibration when compared to the results of Case 1, which is a reasonable result considering that at this DS the structure is expected to be further in the non-linear range. On the other hand, the higher importance of the planar aspect ratio could be related to having a direction significantly weaker than the other, as well as a greater contribution of torsional effects. Once again there is not significant importance of differences in the design code level and the value of β, as could be expected. Again, it is important to consider that these results are specific for the buildings considered in this case study and do not represent the importance of these variables in portfolios with different characteristics, which will be the focus of future studies with wider variability.

4.3 | Case 3: Earthquake Rupture Scenario

Building upon the earlier uniform ground shaking cases to compare the MSA- and IDA-based methods and investigate a simple case to illustrate the basic impacts of correlations, this scenario introduces an earthquake rupture context to explore how structure-to-structure damage correlation impacts damage estimates in a more realistic context. Here, the structure-to-structure damage correlation was estimated based only on the results of IDA on the equivalent SDOF oscillators since the ground motion intensity experienced at each building location was no longer constant and varied spatially, meaning that MSA was no longer feasible (i.e., $im_n \neq im_m$; see Figures 2 and 3). A damage state DS_1 was considered for the analysis, as defined previously. The $Sa_{avg}(T)$ at the respective location of each building was computed for several trials of an assumed earthquake rupture scenario. The shaking was modelled using a suitable GMM and spatial correlation model described below, and after performing Monte Carlo simulations, the probability distribution of the number of damaged buildings was computed as presented in Table 2.

The earthquake rupture scenario was identified from the dominant contributor observed in disaggregation analysis following PSHA (Section 3.3). This was found to be of magnitude $M_w = 6.25$ at a distance of 5 km from the mean building coordinates. The rupture location was thus determined by identifying the closest fault at this distance, resulting in coordinates latitude: 14.3965 and longitude: 41.3958 being selected. The intensity of shaking at each building location was sampled using the GMM proposed by Boore et al. [68]. Here, however, special considerations were made, since the IM adopted for the fragility analysis (Section 3.4) was average spectral acceleration, $Sa_{avg}(T)$, and not $Sa(T)$ estimated by the GMM. To overcome this, the mean and standard deviation of the expected shaking for a given rupture *rup* was estimated indirectly in terms of $Sa_{avg}(T)$ from the $Sa(T)$ estimated by the GMM following the approach proposed by Kohrangi et al. [42] as follows:

$$\mu_{\ln Sa_{avg}(T)|rup} = \frac{1}{N}\sum_{i=1}^{N}\mu_{\ln Sa(T_i)|rup} \tag{11}$$

$$\sigma^2_{\ln Sa_{avg}(T)|rup} = \frac{1}{N^2}\sum_{i=1}^{N}\sum_{j=1}^{N}\rho_{\ln Sa(T_i),\ln Sa(T_j)}\sigma_{\ln Sa(T_i)|rup}\sigma_{\ln Sa(T_j)|rup} \tag{12}$$

where $\mu_{\ln Sa(T_i)|rup}$ and $\sigma^2_{\ln Sa(T_i)|rup}$ are the mean and variance of $Sa(T)$ at a period T_i computed from the GMM, N is the number of periods used to define $Sa_{avg}(T)$, and $\rho_{\ln Sa(T_i),\ln Sa(T_j)}$ is the correlation between periods T_i and T_j computed using the model of Baker and Jayaram [75].

While this approach computes the distribution of shaking in terms of the IM at any given building site location, the spatial correlation between each location's simulated value must also be considered. In the case of $Sa(T)$, this may be considered with spatial correlation models, such as that proposed by Jayaram and Baker [11]. In this study, however, this spatial correlation must be estimated in terms of the IM used in the analysis, $Sa_{avg}(T)$, so the indirect approach proposed by Heresi and Miranda [44] was adopted. It states that the spatial correlation between two sites m and n in terms of $Sa_{avg}(T)$ can be estimated for a given rupture *rup* (whose subscript is dropped herein for brevity) as:

$$\rho_{sp}(m,n) = \frac{\frac{1}{N^2}\sum_{i=1}^{N}\sum_{j=1}^{N}\rho_{\ln Sa(T_i)_m,\ln Sa(T_j)_n}\sigma_{\ln Sa(T_i)_m}\sigma_{\ln Sa(T_j)_n}}{\sigma_{\ln Sa_{avg}(T)_m}\sigma_{\ln Sa_{avg}(T)_n}} \tag{13}$$

where $\sigma_{\ln Sa(T_i)_m}$ is the standard deviation of $Sa(T)$ at a period T_i, computed from the GMM for site location m, and $\sigma_{\ln Sa_{avg}(T)_m}$ is the corresponding standard deviation of $Sa_{avg}(T)$, computed indirectly as previously described. The value of $\rho_{\ln Sa(T_i)_m,\ln Sa(T_j)_n}$ represents the spatial correlation between the spectral ordinates at two periods, i and j, experienced at two different sites, m and n, which was calculated with the Markov model evaluated by Loth and Baker [76]:

$$\rho_{\ln Sa(T_i)_m,\ln Sa(T_j)_n} = \rho_{\ln Sa(T_i),\ln Sa(T_j)}\,\rho_{\ln Sa(T_i)_m,\ln Sa(T_i)_n} \quad \text{with } T_i > T_j \tag{14}$$

where $\rho_{\ln Sa(T_i)_m,\ln Sa(T_i)_n}$ is the spatial correlation between two different sites for the same period, and was estimated from Baker and Jayaram [75].

With this means to estimate ground motion shaking distributions in terms of $Sa_{avg}(T)$, Monte Carlo simulation was used to simulate several trials of the assumed earthquake rupture scenario, as also performed in a recent study by Nafeh and O'Reilly [69]. To illustrate its relative importance in the damage assessment, simulations with and without the spatial correlation were considered. Performing 5000 trials of ground motion shaking, it was found that the estimated mean and median numbers of damaged buildings showed no significant variation, as summarised in Table 7. However, the standard deviation exhibited substantial differences, influencing the distribution tails and the likelihood of exceeding a specific number of damaged buildings other than the mean, consistently with what was found from Scenarios 1 and 2, and as depicted in Figure 11. The findings demonstrate that very different results are obtained when considering only spatial and/or damage correlation, with varying degrees of impact.

What is clear from the plot is that the spatial correlation alone (Case 3.2), when compared to the case where no correlation was considered (Case 3.1), was the most significant impacting factor. When the damage correlation was also considered (Cases 3.3 and 3.4), the curves increased notably but not to the same extent as the number of damaged buildings quickly saturates to the total number of buildings considered within the case study. However, it is important to note that these results are case-specific, where spatial correlation has a strong influence due to the proximity of

TABLE 7 | Statistics on the total number of damaged buildings for cases considered in the earthquake rupture scenario.

Statistic	Case 3.1	Case 3.2	Case 3.3	Case 3.4
Mean	30.5	30.4	30.7	30.4
Median	30.0	31.0	31.0	30.0
Standard deviation	9.5	20.0	13.1	22.8

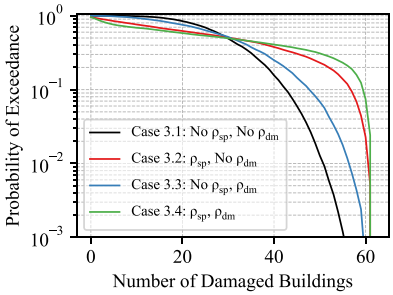

FIGURE 11 | Illustration of the probability of exceeding a given number of damaged buildings for the considered earthquake rupture scenario.

TABLE 8 | Example scenarios of exceedance probabilities for a given number of damaged buildings for the considered earthquake rupture scenario.

Number of buildings	Case 3.1	Case 3.2	Case 3.3	Case 3.4
40	16%	38%	25%	40%
45	6%	31%	15%	36%
50	1%	23%	7%	31%

the studied buildings and is likely the reason for the observed high relative importance of spatial correlation. Scenarios where buildings are more spatially distant could be explored, and the effects of spatial correlation may be less pronounced, and damage correlation could have an even greater impact.

To provide a clearer comparison, Table 8 outlines the probability of exceeding different numbers of damaged buildings across cases, focusing on the range between 40 and 50 buildings, and again the differences are significant. Given that the use of spatial correlation is widely adopted for this type of analysis, Case 3.2 is used as the reference. For instance, focusing on Case 3.4, which considers both spatial and damage correlation, the probability of more than 50 damaged buildings increases from 23% to 31%. It is important to note, however, that the curves for this case presented on Figure 11 both converge rapidly to the total number of buildings in the region (62), meaning that the spatial component is likely dominating, as mentioned previously.

To better understand the real-world implications of this difference, consider a hypothetical scenario in which the local government plans strategies to finance the reconstruction of the three municipalities analysed in this study in the event of an earthquake. Assuming the earthquake scenario presented here is viewed as a 'worst-case scenario,' the government might decide to secure funds to repair the number of buildings with a 20% probability of being damaged by such an event. If the analyst ignored all correlations, they would expect to repair around 38 buildings, and considering just spatial correlation in the risk assessment, this number would increase to 52 buildings. However, if structure-to-structure damage correlation were also considered, as done in this study, the government would need to finance the repair of 57 buildings. Obviously, these numbers are case study specific, and further work could be conducted to examine the impacts in other regions, but the fundamental issue is clear. Additionally, this study only considers situations of residential buildings whose functionality is assumed independent. Analysing structure-to-structure damage correlation in structures such as bridge networks and other lifelines could be much more detrimental from a post-earthquake functionality and indirect loss perspective, although this is beyond the scope of this present study.

5 | Summary and Conclusions

This study presented an analytical method to estimate the *structure-to-structure* damage correlation, based on the assumption that obtaining earthquake induced damage can be modelled as a Bernoulli trial. The method relies on the results of non-linear time-history analyses to estimate the joint probability of damage in pairs of buildings. Two approaches were used: one based on the results of MSA on full 3D models of the buildings with hazard-consistent ground motions, which leads to more accurate characterisation of response but is limited to unrealistic constant shaking cases; and the second based on the results of IDA on equivalent SDOF oscillators, which is computationally more efficient but might yield less accurate results due to the inherent limitations and simplified assumptions of the approach. A case study was conducted on the Caserta Province, Italy, to examine the impact of incorporating *structure-to-structure* correlation on regional damage estimations and to compare the results obtained by the two approaches, particularly with reference to the well-known spatial correlation also considered in regional assessments of this type. Based on this, the following conclusions can be drawn:

- Incorporating *structure-to-structure* damage correlation significantly influences damage estimations in regional risk assessments. While it does not affect considerably the mean or median damage estimates, it heavily impacts the standard deviation, altering the likelihood of exceeding a large number of damaged buildings.
- Using IDA on SDOF oscillators tends to overestimate the total number of damaged buildings compared to the results of using MSA on full 3D models. However, it still performs better than ignoring the correlation entirely. Further research could explore using IDA on full 3D models to improve the accuracy of correlation estimates.
- The current application of the method presented here requires having non-linear models of all the buildings in the studied region, which is information that is generally not available on regional assessments and is not easy to obtain. In addition to that, the computational demand of the methodology poses a significant limitation in using it at a large scale. Future work will focus on integrating this study's findings with the more conventional approach of utilising taxonomy-based fragility functions to ease the computational burden encountered here and further align it with these more widely adopted approaches. Nevertheless, it provides motivation and a foundation for developing mathematical models that estimate correlation directly from certain building characteristics. In order to do that, future studies should focus on assessing the

sufficiency and efficiency of the results and, where possible, validate them against empirical data.

- Incorporating damage correlation allows for more comprehensive scenario-based regional seismic risk assessment, allowing for better planning for seismic mitigation strategies and allocation of funds. In the Caserta Province case study, for instance, including both damage and spatial correlation resulted in a 21.3% increase in estimated buildings to repair, highlighting the importance of accounting for this variable.

Overall, this study presents an advance in modelling for regional seismic risk assessment, demonstrating through a case study the impacts of incorporating structure-to-structure damage correlation on the estimations. Additionally, the method used for estimating the correlation provides a foundation for future developments to account for this variable in a more applicable and efficient way.

Acknowledgements

The work presented in this paper has been developed within the framework of the project "Dipartimenti di Eccellenza 2023–2027," funded by the Italian Ministry of Education, University and Research at IUSS Pavia. The NLTH analyses were carried out on the High Performance Computing DataCenter at IUSS, co-funded by Regione Lombardia through the funding programme established by Regional Decree No. 3776 of November 3, 2020. The ground motion record selections described here were performed using an academic licence of the Djura online ground motion record selector (www.djura.it), and the assistance of Davit Shahnazaryan and Volkan Ozsarac is gratefully acknowledged. The authors would like to thank the comments and suggestions of Prof. Iunio Iervolino and two other anonymous reviewers which greatly improved the paper.

Conflicts of Interest

The authors declare no conflicts of interest.

Data Availability Statement

The data that support the findings of this study are available from the corresponding author upon reasonable request.

Consent

This is to confirm that each of the authors listed, Tomas Mejia and Gerard J. O'Reilly, are aware of this article and have consented to its submission to *Earthquake Engineering* and *Structural Dynamics*.

References

1. C. A. Cornell and H. Krawinkler, "Progress and Challenges in Seismic Performance Assessment," *PEER Center News* 3, no. 2 (2000): 1–2.

2. Federal Emergency Management Agency, Seismic Performance Assessment of Buildings, Volume 1 – Methodology (FEMA P-58), Washington, D.C., 2012.

3. C. A. Cornell, F. Jalayer, R. O. Hamburger, and D. A. Foutch, "Probabilistic Basis for 2000 SAC Federal Emergency Management Agency Steel Moment Frame Guidelines," *Journal of Structural Engineering* 128, no. 4 (2002): 526–533, https://doi.org/10.1061/(ASCE)0733-9445(2002)128:4(526).

4. D. Vamvatsikos, "Accurate Application and Second-Order Improvement of SAC/FEMA Probabilistic Formats for Seismic Performance Assessment," *Journal of Structural Engineering* 140, no. 2 (2014): 04013058, https://doi.org/10.1061/(ASCE)ST.1943-541X.0000774.

5. C. M. Ramirez and E. Miranda, "Building Specific Loss Estimation Methods & Tools for Simplified Performance Based Earthquake Engineering," *John A Blume Earthquake Engineering Center* 171 (2009). Rep.

6. J. Poveda and G. J. O'Reilly, "Seismic Loss Assessment of Existing Hotel Building in Ecuador," *Earthquake Spectra* 41, no. 1 (2024): 955–978, https://doi.org/10.1177/87552930241299356.

7. C. A. Goulet, C. B. Haselton, J. Mitrani-Reiser, et al., "Evaluation of the Seismic Performance of a Code-Conforming Reinforced-Concrete Frame Building—From Seismic Hazard to Collapse Safety and Economic Losses," *Earthquake Engineering & Structural Dynamics* 36, no. 13 (2007): 1973–1997, https://doi.org/10.1002/eqe.694.

8. P. Heresi and E. Miranda, "RPBEE: Performance-Based Earthquake Engineering on a Regional Scale," *Earthquake Spectra* 39, no. 3 (2023): 1328–1351, https://doi.org/10.1177/87552930231179491.

9. L. Bodenmann, J. W. Baker, and B. Stojadinović, "Accounting for Path and Site Effects in Spatial Ground-Motion Correlation Models Using Bayesian Inference," *Natural Hazards and Earth System Sciences* 23, no. 7 (2023): 2387–2402, https://doi.org/10.5194/nhess-23-2387-2023.

10. S. Esposito and I. Iervolino, "PGA and PGV Spatial Correlation Models Based on European Multievent Datasets," *Bulletin of the Seismological Society of America* 101, no. 5 (2011): 2532–2541, https://doi.org/10.1785/0120110117.

11. N. Jayaram and J. W. Baker, "Correlation Model for Spatially Distributed Ground-Motion Intensities," *Earthquake Engineering & Structural Dynamics* 38, no. 15 (2009): 1687–1708, https://doi.org/10.1002/eqe.922.

12. C. Huang, K. Tarbali, and C. Galasso, "A Region-Specific Ground-Motion Model for Inelastic Spectral Displacement in Northern Italy Considering Spatial Correlation Properties," *Seismological Research Letters* 92, no. 3 (2021): 1979–1991, https://doi.org/10.1785/0220200249.

13. S. Ruggieri, F. Porco, G. Uva, and D. Vamvatsikos, "Two Frugal Options to Assess Class Fragility and Seismic Safety for Low-Rise Reinforced Concrete School Buildings in Southern Italy," *Bulletin of Earthquake Engineering* 19, no. 3 (2021): 1415–1439, https://doi.org/10.1007/s10518-020-01033-5.

14. A. Abarca, R. Monteiro, and G. J. O'Reilly, "Seismic Risk Prioritisation Schemes for Reinforced Concrete Bridge Portfolios," *Structure and Infrastructure Engineering* 21, no. 1 (2025): 49–69, https://doi.org/10.1080/15732479.2023.2187424.

15. M. Gaetani d'Aragona, M. Polese, and A. Prota, "Stick-IT: A Simplified Model for Rapid Estimation of IDR and PFA for Existing Low-Rise Symmetric Infilled RC Building Typologies," *Engineering Structures* 223 (2020): 111182, https://doi.org/10.1016/j.engstruct.2020.111182.

16. G. J. O'Reilly and D. Shahnazaryan, "On the Utility of Story Loss Functions for Regional Seismic Vulnerability Modeling and Risk Assessment," *Earthquake Spectra* 40, no. 3 (2024): 1933–1955, https://doi.org/10.1177/87552930241245940.

17. S. Ruggieri, A. Chatzidaki, D. Vamvatsikos, and G. Uva, "Reduced-Order Models for the Seismic Assessment of Plan-Irregular Low-Rise Frame Buildings," *Earthquake Engineering & Structural Dynamics* 51, no. 14 (2022): 3327–3346, https://doi.org/10.1002/eqe.3725.

18. L. Martins and V. Silva, "Development of a Fragility and Vulnerability Model for Global Seismic Risk Analyses," *Bulletin of Earthquake Engineering* 19, no. 15 (2021): 6719–6745, https://doi.org/10.1007/s10518-020-00885-1.

19. M. Giorgio and I. Iervolino, "On Multisite Probabilistic Seismic Hazard Analysis," *Bulletin of the Seismological Society of America* 106, no. 3 (2016): 1223–1234, https://doi.org/10.1785/0120150369.

20. P. Heresi and E. Miranda, "Structure-to-Structure Damage Correlation for Scenario-Based Regional Seismic Risk Assessment,"

Structural Safety 95 (2022): 102155, https://doi.org/10.1016/j.strusafe.2021.102155.

21. Redacción Judicial, "Violaciones a Normas de Sismorresistencia Originaron Colapso de torre 6 del Space: Fiscalía," El Espectador (Sept. 19, 2014). [Online]. Accessed: Jun. 24, 2025. Available: https://www.elespectador.com/judicial/violaciones-a-normas-de-sismorresistencia-originaron-colapso-de-torre-6-del-space-fiscalia-article-517724/.

22. Colprensa, "Ordenan Demolición Total Del edificio Space," El Universal, Jan. 20, 2014. [Online]. Accessed: Jun. 24, 2025. Available: https://www.eluniversal.com.co/colombia/2014/01/20/ordenan-demolicion-total-del-edificio-space/.

23. H. Y. Tamayo Ortiz, "¿Por Qué Derribaron el edificio Bernavento de Medellín?," El Tiempo (Jun. 14, 2018). [Online]. Accessed: Jun. 24, 2025. Available: https://www.eltiempo.com/colombia/medellin/estas-son-las-razones-por-las-cuales-van-a-derribar-el-edificio-bernavento-de-medellin-230242.

24. J. D. Ortiz Jiménez, "Continental Towers, Otro Edificio de CDO Que Será Demolido," El Colombiano (Sept. 17, 2025). [Online]. Accessed: Jun. 24, 2025. Available: https://www.elcolombiano.com/antioquia/continental-towers-otro-edificio-de-cdo-que-sera-demolido-DP18712166.

25. Redacción Nacional, "Ya Son Once los Edificios Construidos por CDO Que Han Sido Sometidos a Estudios," El Espectador, Jul. 12, 2014. [Online]. Accessed: Jun. 24, 2025. Available: https://www.elespectador.com/colombia/medellin/ya-son-once-los-edificios-construidos-por-cdo-que-han-sido-sometidos-a-estudios-article-504513/.

26. J. E. Padgett, R. DesRoches, and E. Nilsson, "Regional Seismic Risk Assessment of Bridge Network in Charleston, South Carolina," *Journal of Earthquake Engineering* 14, no. 6 (2010): 918–933, https://doi.org/10.1080/13632460903447766.

27. V. Silva, H. Crowley, H. Varum, and R. Pinho, "Seismic Risk Assessment for Mainland Portugal," *Bulletin of Earthquake Engineering* 13, no. 2 (2015): 429–457, https://doi.org/10.1007/s10518-014-9630-0.

28. M. Inel, S. M. Senel, S. Toprak, and Y. Manav, "Seismic Risk Assessment of Buildings in Urban Areas: A Case Study for Denizli, Turkey," *Natural Hazards* 46, no. 3 (2008): 265–285, https://doi.org/10.1007/s11069-007-9187-1.

29. R. Lee and A. S. Kiremidjian, "Uncertainty and Correlation for Loss Assessment of Spatially Distributed Systems," *Earthquake Spectra* 23, no. 4 (2007): 753–770, https://doi.org/10.1193/1.2791001.

30. D. J. DeBock, J. W. Garrison, K. Y. Kim, and A. B. Liel, "Incorporation of Spatial Correlations Between Building Response Parameters in Regional Seismic Loss Assessment," *Bulletin of the Seismological Society of America* 104, no. 1 (2014): 214–228, https://doi.org/10.1785/0120130137.

31. C. Kang, O.-S. Kwon, and J. Song, "Evaluation of Correlation Between Engineering Demand Parameters of Structures for Seismic System Reliability Analysis," *Structural Safety* 93 (2021): 102133, https://doi.org/10.1016/j.strusafe.2021.102133.

32. M. Xiang, J. Shen, Z. Xu, and J. Chen, "Structure-to-Structure Seismic Damage Correlation Model," *Earthquake Engineering & Structural Dynamics* 53, no. 10 (2024): 3205–3229, https://doi.org/10.1002/eqe.4172.

33. C. Tsokos and R. Wooten, *The Joy of Finite Mathematics* (Elsevier, 2016), https://doi.org/10.1016/C2014-0-02921-8.

34. D. Vamvatsikos and C. A. Cornell, "Incremental Dynamic Analysis," *Earthquake Engineering & Structural Dynamics* 31, no. 3 (2002): 491–514, https://doi.org/10.1002/eqe.141.

35. F. Jalayer and C. A. Cornell, "Alternative Non-Linear Demand Estimation Methods for Probability-Based Seismic Assessments," *Earthquake Engineering & Structural Dynamics* 38, no. 8 (2009): 951–972, https://doi.org/10.1002/eqe.876.

36. M. Kohrangi, D. Vamvatsikos, and P. Bazzurro, "Site Dependence and Record Selection Schemes for Building Fragility and Regional Loss Assessment," *Earthquake Engineering & Structural Dynamics* 46, no. 10 (2017): 1625–1643, https://doi.org/10.1002/eqe.2873.

37. J. W. Baker, "Measuring Bias in Structural Respinse Caused by Ground Motion Scaling," in Proc. 8th Pacific Conf. on Earthquake Engineering, Singapore, (2007).

38. H. Dávalos and E. Miranda, "A Ground Motion Prediction Model for Average Spectral Acceleration," *Journal of Earthquake Engineering* 25, no. 2 (2021): 319–342, https://doi.org/10.1080/13632469.2018.1518278.

39. G. J. O'Reilly, "Limitations of Sa(T1) as an Intensity Measure When Assessing Non-Ductile Infilled RC Frame Structures," *Bulletin of Earthquake Engineering* 19, no. 6 (2021): 2389–2417, https://doi.org/10.1007/s10518-021-01071-7.

40. S. Aristeidou and G. J. O'Reilly, "Exploring the Use of Orientation-Independent Inelastic Spectral Displacements in the Seismic Assessment of Bridges," *Journal of Earthquake Engineering* 28, no. 12 (2024): 3515–3538, https://doi.org/10.1080/13632469.2024.2343067.

41. L. Eads, E. Miranda, and D. G. Lignos, "Average Spectral Acceleration as an Intensity Measure for Collapse Risk Assessment," *Earthquake Engineering & Structural Dynamics* 44, no. 12 (2015): 2057–2073, https://doi.org/10.1002/eqe.2575.

42. M. Kohrangi, S. R. Kotha, and P. Bazzurro, "Ground-Motion Models for Average Spectral Acceleration in a Period Range: Direct and Indirect Methods," *Bulletin of Earthquake Engineering* 16, no. 1 (2018): 45–65, https://doi.org/10.1007/s10518-017-0216-5.

43. S. Aristeidou, D. Shahnazaryan, and G. J. O'Reilly, "Artificial Neural Network-Based Ground Motion Model for Next-Generation Seismic Intensity Measures," *Soil Dynamics and Earthquake Engineering* 184 (2024): 108851, https://doi.org/10.1016/j.soildyn.2024.108851.

44. P. Heresi and E. Miranda, "Intensity Measures for Regional Seismic Risk Assessment of Low-Rise Wood-Frame Residential Construction," *Journal of Structural Engineering* 147, no. 1 (2021): 04020138, 10.1061/(ASCE)ST.1943-541X.0002859.

45. A. Suzuki and I. Iervolino, "Intensity Measure Conversion of Fragility Curves," *Earthquake Engineering & Structural Dynamics* 49, no. 6 (2020): 607–629, https://doi.org/10.1002/eqe.3256.

46. A. M. B. Nafeh, G. J. O'Reilly, and R. Monteiro, "Simplified Seismic Assessment of Infilled RC Frame Structures," *Bulletin of Earthquake Engineering* 18, no. 4 (2020): 1579–1611, https://doi.org/10.1007/s10518-019-00758-2.

47. L. J. Emrich and M. R. Piedmonte, "A Method for Generating High-Dimensional Multivariate Binary Variates," *American Statistician* 45, no. 4 (1991): 302–304, https://doi.org/10.2307/2684460.

48. V. Ozsarac, N. Pereira, H. Mohamed, X. Romão, and G. J. O'Reilly, "The Built Environment Data Framework for Simulated Design and Vulnerability Modelling in Earthquake Engineering," *Earthquake Engineering & Structural Dynamics* 54 (2025): 2651–2670, https://doi.org/10.1002/eqe.4378.

49. V. Corlito and G. D. Matteis, "Caratterizzazione Tipologico-strutturale e Valutazione Della vulnerabilità sismica degli edifici in cemento armato della provincia di caserta attraverso i, parametri Della Scheda cartis," in *XVIII CONVEGNO ANIDIS "L'Ingegneria Sismica inItalia*, 96–104, Pisa University Press srl, (2019).

50. *Norme Tecniche per le Costruzioni*, Decreto Ministeriale 17 gennaio 2018, Ministero Delle Infrastrutture e Dei Trasporti, Italy (2018).

51. H. Crowley, V. Despotaki, D. Rodrigues, et al., "European Exposure Model Data Repository (v1.0) [Data set]," *Zenodo* (2021), https://doi.org/10.5281/zenodo.5730071.

52. GEM. "gem_taxonomy." GitHub. Accessed: Apr. 7, 2025. Available: https://github.com/gem/gem_taxonomy.

53. GEMScienceTools. "spatial-disaggregation." GitHub. Accessed: Apr. 7, 2025. Available: https://github.com/GEMScienceTools/spatial-disaggregation.

54. WorldPop (www.worldpop.org—School of Geography and Environmental Science, University of Southampton) and Center for International Earth Science Information Network (CIESIN), Columbia University (2018). The spatial distribution of population in 2018 with country total adjusted to match the corresponding UNPD estimate, China. DOI: 10.5258/SOTON/WP00660.

55. H. Crowley, V. Despotaki, V. Silva, et al., "Model of Seismic Design Lateral Force Levels for the Existing Reinforced Concrete European Building Stock," *Bulletin of Earthquake Engineering* 19, no. 7 (2021): 2839–2865, https://doi.org/10.1007/s10518-021-01083-3.

56. M. Zhu, F. McKenna, and M. H. Scott, "OpenSeesPy: Python Library for the OpenSees Finite Element Framework," *SoftwareX* 7 (2018): 6–11, https://doi.org/10.1016/j.softx.2017.10.009.

57. F. Zareian and R. A. Medina, "A Practical Method for Proper Modeling of Structural Damping in Inelastic Plane Structural Systems," *Computers and Structures* 88, no. 1–2 (2010): 45–53, https://doi.org/10.1016/j.compstruc.2009.08.001.

58. T. Panagiotakos and M. Fardis, "Deformations of Reinforced Concrete Members at Yielding and Ultimate," *ACI Structural Journal* 98, no. 2 (2001): 135–148, https://doi.org/10.14359/10181.

59. "EN 1998-3: Eurocode 8: Design of Structures for Earthquake Resistance — Part 3: Assessment and Retrofitting of Buildings", EN 1998-3:2005, European Committee for Standardization (2005).

60. C. B. Haselton, A. B. Liel, S. C. Taylor-Lange, and G. G. Deierlein, "Calibration of Model to Simulate Response of Reinforced Concrete Beam-Columns to Collapse," *ACI Structural Journal* 113, no. 6 (2016): 1141–1152, https://doi.org/10.14359/51689245.

61. *Seismic Evaluation and Retrofit of Existing Buildings, Standard ASCE/SEI 41-17*, American Society of Civil Engineers, Reston, VA, USA, 2017.

62. K. J. Elwood and J. P. Moehle, "Shake Table Tests and Analytical Studies on the Gravity Load Collapse of Reinforced Concrete Frames," Pacific Earthquake Engineering Research Center, University of California, Berkeley, PEER Rep. 2003/01 (2003).

63. K. J. Elwood, "Modelling Failures in Existing Reinforced Concrete Columns," *Canadian Journal of Civil Engineering* 31, no. 5 (2004): 846–859, https://doi.org/10.1139/l04-040.

64. H. Sezen and J. P. Moehle, "Shear Strength Model for Lightly Reinforced Concrete Columns," *Journal of Structural Engineering* 130, no. 11 (2004): 1692–1703, https://doi.org/10.1061/(ASCE)0733-9445(2004)130:11(1692).

65. G. J. O'Reilly, *Performance-Based Seismic Assessment and Retrofit of Existing RC Frame Buildings in Italy* (Pavia, Italy: Scuola Universitaria Superiore, IUSS Pavia, 2016), Ph.D. dissertation, 10.13140/RG.2.2.32605.97761.

66. G. J. O'Reilly and T. J. Sullivan, "Modeling Techniques for the Seismic Assessment of the Existing Italian RC Frame Structures," *Journal of Earthquake Engineering* 23, no. 8 (2019): 1262–1296, https://doi.org/10.1080/13632469.2017.1360224.

67. J. Woessner, D. Laurentiu, D. Giardini, et al., "The 2013 European Seismic Hazard Model: Key Components and Results," *Bulletin of Earthquake Engineering* 13, no. 12 (2015): 3553–3596, https://doi.org/10.1007/s10518-015-9795-1.

68. D. M. Boore, J. P. Stewart, E. Seyhan, and G. M. Atkinson, "NGA-West2 Equations for Predicting PGA, PGV, and 5% Damped PSA for Shallow Crustal Earthquakes," *Earthquake Spectra* 30, no. 3 (2014): 1057–1085, https://doi.org/10.1193/070113EQS184M.

69. A. M. B. Nafeh and G. J. O'Reilly, "Fragility Functions for Non-Ductile Infilled Reinforced Concrete Buildings Using Next-Generation Intensity Measures Based on Analytical Models and Empirical Data From Past Earthquakes," *Bulletin of Earthquake Engineering* 22 (2024): 4983–5021, https://doi.org/10.1007/s10518-024-01955-4.

70. M. Kohrangi, P. Bazzurro, D. Vamvatsikos, and A. Spillatura, "Conditional Spectrum-Based Ground Motion Record Selection Using Average Spectral Acceleration," *Earthquake Engineering & Structural Dynamics* 46, no. 10 (2017): 1667–1685, https://doi.org/10.1002/eqe.2876.

71. M. Kohrangi, D. Vamvatsikos, and P. Bazzurro, "Implications of Intensity Measure Selection for Seismic Loss Assessment of 3-D Buildings," *Earthquake Spectra* 32, no. 4 (2016): 2167–2189, https://doi.org/10.1193/112215EQS177M.

72. T. Lin, C. B. Haselton, and J. W. Baker, "Conditional Spectrum-Based Ground Motion Selection. Part I: Hazard Consistency for Risk-Based Assessments," *Earthquake Engineering & Structural Dynamics* 42, no. 12 (2013): 1847–1865, https://doi.org/10.1002/eqe.2301.

73. I. Iervolino, G. Manfredi, M. Polese, G. M. Verderame, and G. Fabbrocino, "Seismic Risk of R.C. Building Classes," *Engineering Structures* 29, no. 5 (2007): 813–820, https://doi.org/10.1016/j.engstruct.2006.06.019.

74. L. Martins, V. Silva, H. Crowley, and F. Cavalieri, "Vulnerability Modellers Toolkit, an Open-Source Platform for Vulnerability Analysis," *Bulletin of Earthquake Engineering* 19, no. 13 (2021): 5691–5709, https://doi.org/10.1007/s10518-021-01187-w.

75. J. W. Baker and N. Jayaram, "Correlation of Spectral Acceleration Values From NGA Ground Motion Models," *Earthquake Spectra* 24, no. 1 (2008): 299–317, https://doi.org/10.1193/1.2857544.

76. C. Loth and J. W. Baker, "A spatial Cross-Correlation Model of Spectral Accelerations at Multiple Periods," *Earthquake Engineering & Structural Dynamics* 42, no. 3 (2013): 397–417, https://doi.org/10.1002/eqe.2212.